

1 Identification of clinically-relevant genetic alterations in 2 uveal melanoma using RNA sequencing

3 R.J. Nell¹

4 M. Versluis¹

5 D. Cats⁴

6 H. Mei⁴

7 R.M. Verdijk^{2,3}

8 W.G.M. Kroes⁵

9 G.P.M. Luyten¹

10 M.J. Jager¹

11 P.A. van der Velden^{1*}

12

13 ¹ Department of Ophthalmology, Leiden University Medical Center, Leiden, the Netherlands.

14 ² Department of Pathology, Leiden University Medical Center, Leiden, the Netherlands.

15 ³ Department of Pathology, Erasmus University Medical Center, Rotterdam, the Netherlands.

16 ⁴ Department of Biomedical Data Sciences, Leiden University Medical Center, Leiden, the
17 Netherlands.

18 ⁵ Department of Clinical Genetics, Leiden University Medical Center, Leiden, the
19 Netherlands.

20

21 * Corresponding author, Department of Ophthalmology, Leiden University Medical Center,
22 PO Box 9600, 2300 RC Leiden, The Netherlands.

23

24 Acknowledgements

25 This study is supported by the European Union's Horizon 2020 research and innovation
26 program under grant agreement number 667787 (UM Cure 2020, Rogier J. Nell). We thank
27 Ronald van Eijk (Department of Pathology, Leiden University Medical Center, Leiden, the
28 Netherlands) for his help with the *BAP1* DNA sequencing experiments. This work is partly
29 based upon data generated by The Cancer Genome Atlas (TCGA) Research Network:

30 <https://www.cancer.gov/tcga>.

31 **Abstract**

32 **Introduction**

33 Uveal melanoma is a lethal intraocular tumour, in which the presence of certain genetic
34 alterations correlates with the risk of metastatic dissemination and patient survival. RNA data
35 is typically used to transcriptionally characterise tumours and their micro-environment. In this
36 study, we tested the detectability of all key genetic alterations in uveal melanoma from RNA
37 sequencing data.

38

39 **Methods**

40 Cohort-wide gene expression profiling was used to classify tumours at the transcriptional
41 level. In individual samples, copy number alterations affecting chromosomes 3 and 8q were
42 analysed by measuring expressed allelic imbalances of heterozygous common single
43 nucleotide polymorphisms. Mutations in *GNAQ*, *GNA11*, *CYSLTR2*, *PLCB4*, *BAP1*, *SF3B1*
44 and *EIF1AX* were identified by screening of hotspot regions and by evaluating their
45 transcriptional effects. All findings were cross-validated with DNA-derived data in a training
46 cohort of 80 primary uveal melanomas studied by The Cancer Genome Atlas (TCGA)
47 initiative, and in five prospectively analysed cases from our institution.

48

49 **Results**

50 Unsupervised gene expression profiling strongly correlated to the presence of chromosome
51 3 alterations, but was not reliable in identifying other (clinically-)relevant genetic alterations.
52 However, the presence of both chromosome 3 and 8q copy number alterations could be
53 successfully inferred from expressed allelic imbalances in most tumours. The majority of
54 mutations were adequately recognised at the RNA level by their nucleotide changes (all
55 genes), alternative splicing around the mutant position (*BAP1*) and transcriptome-wide
56 aberrant splice junction usage (*SF3B1*). Notably, in the TCGA cohort we detected previously
57 unreported mutations in *BAP1* (n=3) and *EIF1AX* (n=5), that were missed by the original
58 DNA sequencing. In our prospective cohort, all mutations and copy number alterations were
59 successfully identified at the RNA level by combining the described approaches.

60

61 **Conclusion**

62 In addition to providing gene expression levels and profiles, RNA from uveal melanomas
63 presents insights into the expressed tumour genotype and its phenotypic consequences.
64 Such complete analysis of transcriptional data may augment or even substitute current DNA-
65 based approaches, and has potential applicability in both research and clinical practice.

66 Introduction

67 Uveal melanoma is a lethal intraocular tumour characterised by a high metastatic rate and
68 limited treatment options once disseminated [1]. In contrast to most other malignancies, it
69 presents as a relatively simple genetic disease with a low mutational burden and limited
70 number of structural variants [2, 3]. Practically all tumours harbour a mutually-exclusive
71 mutation in *GNAQ*, *GNA11*, *CYSLTR2* or *PLCB4*, which activates the $G\alpha_q$ signalling
72 pathway [4-7]. Most uveal melanomas also carry a so-called BSE (*BAP1*, *SF3B1* or *EIF1AX*)
73 mutation [2, 8-10]. Copy number losses of chromosome 3 and increases of chromosome 8q
74 are the most prevalent structural alterations, and occur in specific combinations together with
75 the BSE mutations. These various molecular subtypes have been associated with distinct
76 gene expression profiles (GEP) and are differentially correlated to the risk of early metastatic
77 dissemination and consequent patient survival (**Table 1**) .

78

79 The prognostic value of genetic alterations in uveal melanoma has been recognised for more
80 than two decades. Traditionally, copy number alterations were studied using cytogenetic
81 techniques, such as karyotyping, fluorescence in situ hybridisation, multiplex ligation-
82 dependent probe amplification and array genotyping [11-15]. Technical advancements
83 enabled genome-wide analyses by next-generation sequencing and led to the discovery of
84 recurrent mutations [2, 8-10]. Nowadays, (targeted) sequencing can be used to detect all
85 relevant alterations – both copy number alterations and mutations – in one single analysis
86 [16, 17].

87

88 In addition to these DNA-based approaches, several studies have identified clinically-
89 relevant transcriptional subtypes of uveal melanoma [18-21]. Most commonly, tumours are
90 divided into class I or II based on their bulk GEP. This classification can be established using
91 dimensionality reduction and sample clustering techniques of total RNA expression data, or
92 by evaluating expression variation in a selection of genes. Intriguingly, this transcriptional
93 classification of tumours is known to strongly correlate with the presence of genetic
94 alterations affecting chromosome 3 (**Table 1**). Given that part of the bulk GEP may be
95 derived from admixed non-malignant cells, such as tumour-infiltrating immune cells, RNA
96 data can also provide insights into the tumour microenvironment of uveal melanomas [22,
97 23].

98

99 More recently, the presence and consequences of genetic alterations at the transcriptional
100 level have gained interest in the context of uveal melanoma. Mutations in *SF3B1*, a gene
101 encoding for a core component of the cell's splicing machinery, were found to lead to a

102 recurrent profile of aberrant splice junction usage [2, 24]. As another example, in three large-
103 scale genomic studies, a variety of complex *BAP1* alterations were only identified after using
104 RNA sequencing data in addition to DNA-derived data [21, 25, 26]. Finally, *CYSLTR2* mutant
105 uveal melanomas recurrently showed silencing of the wild-type allele and preferential
106 expression of the p.L129Q mutation [27]. These examples emphasise the value of
107 investigating RNA in addition to DNA to identify the presence and consequences of certain
108 genetic alterations.

109
110 In this study, we apply various bioinformatic approaches to detect all key genetic alterations
111 in uveal melanoma by only using tumour-derived RNA sequencing data. Cohort-wide GEP is
112 used to identify class I and II tumours. In individual samples, copy number alterations are
113 analysed by measuring expressed allelic imbalances of heterozygous common single
114 nucleotide polymorphisms (SNPs). Mutations are identified by screening of hotspot regions
115 and by evaluating their transcriptional effects. Our findings are cross-validated with DNA-
116 derived data in a training cohort of 80 primary uveal melanomas originally studied by The
117 Cancer Genome Atlas (TCGA) initiative, and in five prospectively analysed cases from our
118 institution.

119 **Methods**

120 **Collection and analysis of retrospective cohort**

121 RNA sequencing files from the 80 primary uveal melanomas studied by the TCGA [13] were
122 downloaded from the NCI Genomic Data Commons data portal (GDC;
123 <https://portal.gdc.cancer.gov>). After reconversion to FASTQ files using samtools (version
124 1.1), the reads were aligned using STAR (version 2.5.3a) to human reference genome
125 GRCh38. Gene counts were generated using htseq-count (version 0.6.0) and annotated with
126 Ensembl (version 87). DESeq2 (version 1.30.0) was used for variance stabilising
127 transformation of the count data, which formed the input for the uniform manifold
128 approximation and projection (UMAP) analysis. An expression signature of 200 genes
129 characterising the two visually separated clusters was identified using ClaNC, and was used
130 to classify tumours as 'class I' or 'class II' based on the relative expression of chromosome 3
131 genes (i.e. high or low, respectively).

132
133 The aligned RNA sequencing files were analysed for variants using VarScan (version 2.3),
134 which were annotated using snpEff/snpSift (version 5.1) according to dbSNP (version 151).
135 Only heterozygously and highly expressed common SNPs (flagged as 'common', total
136 number of reads > 40, number of reference reads > 2, number of alternate reads > 2) were
137 included in the downstream analysis. For all SNPs, the fractions alternate reads of total
138 reads were visualised according to their chromosomal positions. Segmentation was
139 performed manually. RNA-derived allelic (im)balances were compared to DNA-measured
140 copy number information determined from Affymetrix SNP 6.0 arrays, available from the
141 Pan-Cancer Atlas initiative [28].

142
143 All aligned RNA sequencing files were further screened for (hotspot) mutations in *GNAQ*
144 (p.Q209, p.R183 and p.G48), *GNA11* (p.Q209, p.R183), *CYSLTR2* (p.L129), *PLCB4*
145 (p.D630), *EIF1AX* (entire gene), *SF3B1* (exon 14) and *BAP1* (entire gene) using freebayes
146 (version 1.3.6), and via manual inspection using the Integrative Genomics Viewer (version
147 2.8.10). The presence of mutations was compared to those detectable in aligned DNA
148 sequencing files generated by exome-captured sequencing (n=80) or low-pass whole-
149 genome sequencing (n=51) downloaded from the GDC data portal.

150
151 The bioinformatic analyses were carried out using R (version 4.0.3) and RStudio (version
152 1.4.1103). All custom scripts are available via <https://github.com/rjnell/um-rna>.

153

154 **Collection, isolation and analysis of prospective cohort**

155 Five snap-frozen primary uveal melanoma specimens were collected from the biobank of the
156 Department of Ophthalmology, Leiden University Medical Center (LUMC). These samples
157 were originally obtained from patients treated by an enucleation in the LUMC. This study
158 was approved by the LUMC Biobank Committee and Medisch Ethische Toetsingscommissie
159 under numbers B14.003/SH/sh and B20.026/KB/kb.

160

161 RNA from all specimens (25x 20µm sections) was isolated using the QIAamp RNeasy Mini
162 Kit (Qiagen, Hilden, Germany), following the manufacturer's instructions. 100 ng of RNA per
163 sample was sequenced by GenomeScan (Leiden, the Netherlands). Sample preparation
164 was performed using the NEBNext Ultra Directional RNA Library Prep Kit for Illumina (New
165 England Biolabs, Ipswich, USA) according to the NEB #E7240S/L protocol. In short, mRNA
166 was isolated from total RNA using oligo-dT magnetic beads. After fragmentation of the
167 mRNA, cDNA synthesis was performed and used for ligation with the sequencing adapters
168 and PCR amplification. Quality and yield were measured with the Fragment Analyzer
169 (Agilent, Santa Clara, USA). Next, clustering and DNA sequencing was performed using the
170 cBot and HiSeq 4000 (Illumina, San Diego, USA) according to the manufacturer's protocols.
171 HiSeq control and image analysis, base calling and quality check were carried out using
172 HCS (version 3.4.0), the Illumina data analysis pipeline RTA (version 2.7.7) and bcl2fastq
173 (version 2.17). The raw sequencing files underwent the same alignment and analysis
174 pipeline as the TCGA data files to perform GEP clustering and infer copy number alterations
175 and mutations.

176

177 DNA from uveal melanomas (25x 20µm sections) was isolated with the QIAamp DNA Mini Kit
178 (Qiagen) according to the manufacturer's instructions. Digital PCR was performed to
179 measure the copy number values of chromosome 3 and 8q and to confirm mutations in
180 *GNAQ*, *GNA11*, *EIF1AX* and *SF3B1*. These experiments were carried out using the QX200
181 Droplet Digital PCR System (Bio-Rad Laboratories, Hercules, USA) following established
182 protocols [22, 27, 29-31], and two new assays listed in **Supplementary Table 1**. The
183 presence and pathogenicity of *BAP1* alterations was confirmed by targeted Sanger or next-
184 generation sequencing and an immunohistochemical staining, both performed as routine
185 diagnostic analyses in two ISO accredited laboratories (Departments of Clinical Genetics
186 and Pathology, LUMC) [16, 32].

187

188 Results

189 Estimation of genetic alterations via cohort-wide gene expression profiling

190 The RNA-derived classification of primary uveal melanomas into GEP class I or II is
191 originally based on unsupervised clustering of transcriptome-wide expression data into two
192 groups [19, 20]. Concordantly, a dimensionality reduction analysis (UMAP) successfully
193 divided the TCGA tumours (n=80) into two main clusters based on their total transcriptional
194 diversity (**Figure 1A**). To investigate expression patterns underlying this subdivision, we
195 inferred a signature of 200 genes characterising the two clusters. The largest proportion
196 (82/200, 41%) of these genes were located on chromosome 3 (**Figure 1B and**
197 **Supplementary Table 2**), with systematically lower levels of expression in one cluster of
198 tumours (n=40, marked as GEP class II) relative to the other (n=40, marked as GEP class I).
199 This classification almost completely overlapped with the true DNA-determined copy number
200 status of chromosome 3: 40/40 GEP class II tumours demonstrated loss of this chromosome
201 (i.e. monosomy, or isodisomy in polyploid melanomas), compared to 3/40 GEP class I
202 tumours (**Figure 1C and Supplementary Table 3**). The three discordant cases were the
203 only tumours showing arm-level variation of chromosome 3 loss (n=2) or an unusual trisomy
204 3 in the context of polyploidy (n=1, **Supplementary Figure 1A and B**). In line with the
205 frequent co-occurrence of chromosome 3 copy number losses and *BAP1* alterations,
206 mutations in *BAP1* were present in 40/40 GEP class II and 0/40 GEP class I tumours
207 (**Figure 1C and Supplementary Table 3**).

208
209 In contrast, cohort-wide GEP clustering did not specifically overlap with the presence of
210 chromosome 8q copy number changes or other mutations, even not after specifying the
211 analysis to class I or II tumours only (**Figure 1C and Supplementary Figure 2**). These
212 observations suggest that alternative approaches are needed to infer all (clinically-)relevant
213 genetic alterations from RNA data.

215 Identification of copy number alterations via RNA-expressed allelic imbalances

216 To detect chromosomal copy number alterations in individual tumours, we proceeded by
217 measuring regional allelic imbalances in the RNA sequencing data. For this goal, highly
218 expressed heterozygous common SNPs were identified and their so-called B-allele fractions
219 (BAFs) were visualised according to their chromosomal positions. These values refer to the
220 measured expression of one allele compared to the total expression of both alleles. Under
221 copy number neutral conditions, two alleles – and thus both SNP variants – are equally

222 abundant, resulting in BAFs of ~50% (**Figure 2A**). In contrast, a chromosomal loss, such as
223 monosomy 3, typically leads to BAFs close to ~0% and ~100%, as it is caused by an
224 (almost) complete loss of one of the two alleles ('loss of heterozygosity', **Figure 2B**). Using
225 this approach, we were able to correctly identify disomic tumours (n=40, with preserved
226 balanced expression) and tumours with (partial) loss of chromosome 3 (n=39, showing
227 imbalanced expression) from the RNA sequencing data in 79/80 (99%) cases of the TCGA
228 cohort (**Figure 2C and Supplementary Table 3**). The only conflicting case was the one
229 presenting with an unusual trisomy 3 in the context of polyploidy, which was also
230 characterised by an allelic imbalance (**Supplementary Figure 1B**).

231
232 This latter case illustrates that, similar to chromosomal losses, copy number increases
233 typically also lead to allelic imbalances. A gain, such as of chromosome 8q (or chromosome
234 3 in the discordant case described above), is usually the result of an extra copy of one allele,
235 leading to BAFs around ~67% and ~33% (**Figure 2A**). Larger amplifications mostly originate
236 from several copies of one allele (with BAFs >67% and <33%, **Figure 2B**). On the other
237 hand, amplifications derived from extra copies of both alleles or subclonal alterations result
238 in BAFs closer to 50% and may be more difficult to recognise (**Supplementary Figure 1C**).
239 In the TCGA cohort, chromosome 8q allelic imbalances were detected in the RNA
240 sequencing data of 53 tumours, which all had a DNA-confirmed gain or amplification of
241 chromosome 8q. The remaining 27 cases lacked measurable BAF deviations, and could be
242 explained by a disomy 8q (n=21) or a copy number increase of both alleles (n=6). In
243 aggregate, the presence or absence of any 8q alteration was correctly identified from RNA
244 sequencing data in 74/80 (93%) of these uveal melanomas (**Figure 2C and Supplementary**
245 **Table 3**).

246
247 Of note, depending on the number of informative SNPs and their clonality in individual
248 tumours, regional allelic imbalances involving other chromosomes were also successfully
249 identified by this approach (**Figure 2A and B**).

250

251 **RNA-based identification of G α_q and BSE mutations**

252 Next, we aimed to identify the mutational status of individual uveal melanomas at the
253 transcriptional level (**Figure 3A and Supplementary Table 3**). G α_q signalling mutations are
254 known to occur at a selected number of hotspots (p.G48, p.R183 and p.Q209 for *GNAQ* and
255 *GNA11*, p.L129 for *CYSLTR2* and p.D630 for *PLCB4* [4-7]), allowing for a targeted analysis
256 of RNA sequencing data (**Figure 3B**). Though, due to a lack of sequencing reads covering
257 the mutant positions, DNA-confirmed *GNAQ* mutations could not be adequately detected in

258 the RNA data of four cases (**Supplementary Figure 2A**). Still, the $G\alpha_q$ mutations were
259 correctly identified in the remaining 74/78 (95%) mutant uveal melanomas (**Figure 3A and**
260 **Supplementary Table 3**).

261

262 *BAP1* alterations are typically inactivating mutations (or deletions) that can be present
263 throughout the complete *BAP1* gene. This challenges the identification of all alterations
264 using conventional sequencing [25, 26]. In the TCGA cohort of uveal melanomas, it was
265 earlier shown that various complex (intronic) *BAP1* alterations can be identified by the use of
266 RNA sequencing [21, 25]. Importantly, exonic missense and nonsense mutations are also
267 detectable at the transcriptional level: directly via their nucleotide changes, or indirectly via
268 observed alternative splicing events such as (partial) intron retention or exon skipping
269 (**Figure 3C**). Due to a low number of mutant RNA sequencing reads, two mutations were
270 only identified at the DNA level (**Supplementary Figure 2A**). Taken together, 38/40 (95%)
271 *BAP1* mutations could be detected via RNA sequencing (**Figure 3A and Supplementary**
272 **Table 3**), including three mutations that had remained unrecognised in previous studies
273 (p.W196X in VD-A8KM, a deletion involving the start of exon 1 in V4-A9ES, and a frameshift
274 deletion involving exon 8 in WC-A883, **Figure 3C and Supplementary Figure 2B**).

275

276 *SF3B1* mutations in uveal melanomas are predominantly found in exon 14, with most of
277 them affecting positions p.R625 or p.K666 [2, 9, 10, 24]. We successfully identified 14/15
278 (93%) DNA-confirmed mutations by nucleotide variation in the RNA sequencing data of the
279 TCGA cohort (**Figure 3A, 3D and Supplementary Table 3**), with again a limited number of
280 reads at the mutant position in the discordant tumour (**Supplementary Figure 2A**).

281 However, alternative splicing was found in all 15/15 (100%) mutant tumour samples (**Figure**
282 **3E**), corroborating the differences between *SF3B1* mutant and wild-type uveal melanomas at
283 the RNA level [24].

284

285 *EIF1AX* mutations mainly affect the N-terminal region of the gene, spanning the first two
286 exons with a total of fifteen amino acids [10]. In the TCGA dataset, we detected the
287 presence of a DNA-confirmed *EIF1AX* mutation in the RNA of 9/10 tumours, with – similar to
288 the missed *GNAQ* mutation in the same tumour – a lack of sequencing reads explaining the
289 discordant sample (**Supplementary Figure 2A**). However, we also observed that there was
290 practically no coverage of exon 1 in the exome-captured DNA sequencing data, and none of
291 the TCGA tumours was known to have an exon 1 mutation [21]. By analysing the
292 (uncaptured) RNA sequencing data (**Figure 3D**), we identified expressed exon 1 mutations
293 in five TCGA cases (p.P2H in VD-AA8M, p.P2L in YZ-A983, p.P2R in V4-A9EH, p.K3N in
294 WC-A87T, and p.N4S in VD-AA8Q). All these tumours further presented with disomy of

295 chromosomes 3 and 8q and lacked mutations in *SF3B1* or *BAP1*, in line with the typical
296 genotype of *EIF1AX*-mutant tumours. For two cases, low-pass whole genome sequencing
297 was available and confirmed both mutations (**Supplementary Figure 2C**). Taken together,
298 14/15 (93%) *EIF1AX* mutations were successfully identified at the RNA level, including five
299 previously missed with DNA-based exome sequencing (**Figure 3A and Supplementary**
300 **Table 3**).

301

302 **Prospective validation of RNA-based detectability of genetic alterations**

303 Finally, we aimed to prospectively validate all beforementioned techniques in an
304 independent cohort. For this goal, we performed RNA sequencing of five primary uveal
305 melanoma specimens obtained after enucleation in our hospital (**Figure 4 and**
306 **Supplementary Table 4**). The presence of chromosome 3 and 8q copy number alterations,
307 and $G\alpha_q$ and BSE mutations was confirmed at the DNA level using digital PCR and targeted
308 sequencing, and – for *BAP1* – at the protein level using immunohistochemistry.

309

310 Although the number of tumours in our cohort was too low to reliably determine the GEP
311 classification based on unsupervised clustering (**Figure 4A**), three tumours were found to be
312 GEP class I and two tumours were GEP class II upon evaluation of our TCGA-based 200-
313 gene expression signature. This classification matched with the loss of heterozygosity of
314 chromosome 3 in the RNA sequencing data (exemplified in **Figure 4B**). Additionally, three
315 tumours showed allelic imbalances of chromosome 8q. The presence of all these presumed
316 copy number alterations could be successfully validated at the DNA level.

317

318 Regarding the $G\alpha_q$ mutations, all five tumours expressed one hotspot mutation in *GNAQ*
319 (n=4) or *GNA11* (n=1, **Figure 4B**). Next, the RNA data demonstrated the presence of BSE
320 mutations in *BAP1* (n=2), *SF3B1* (n=2) and *EIF1AX* (n=1). The *BAP1* mutations caused
321 RNA-detectable nucleotide variation as well as altered splicing around the mutated sites,
322 showing high similarities to TCGA tumours with comparable mutations (**Figure 4C**). The
323 tumours with the *SF3B1* p.R625 hotspot mutations were the ones demonstrating *SF3B1*-
324 associated aberrant splicing (**Figure 4D**). One tumour carried an *EIF1AX* mutation affecting
325 exon 2. All mutations could be verified at the DNA level. Additionally, the presence and
326 pathogenicity of the *BAP1* alterations was supported by a negative (n=2) or positive (n=3)
327 *BAP1* nuclear staining (**Supplementary Table 4**).

328

329 Taken together, all measured copy number alterations and mutations were correctly
330 identified in the RNA sequencing data of the five uveal melanomas.

331 Discussion

332 Uveal melanoma is characterised by a number of prognostically-relevant combinations of
333 genetic alterations, that are mostly measured at the DNA level. In this study, we tested
334 whether these alterations could also be detected at the transcriptional level using RNA
335 sequencing data. This identification of mutations and copy number alterations was cross-
336 validated with DNA-based techniques in both a retrospective cohort of 80 TCGA tumours
337 and five prospectively analysed uveal melanomas from our own cohort.

338

339 First of all, we explored the indirect detectability of genetic alterations via unsupervised GEP
340 clustering, a commonly-used procedure in the context of classifying uveal melanoma. Our
341 analysis revealed – in line with earlier studies – two main groups of tumours which
342 overlapped with the absence or presence of chromosome 3 alterations (complete
343 chromosomal loss and *BAP1* mutation, **Figure 1 and 4A**). Indeed, a large number of genes
344 on chromosome 3 was expressed systematically lower in bulk RNA upon loss of this
345 chromosome. However, GEP clustering was influenced by the extent of chromosome 3 loss
346 (i.e. partial losses were not identified) and could not be used to specify the exact *BAP1*
347 mutation. It also did not identify chromosome 8q copy number alterations or any of the other
348 recurrent and relevant mutations, such as those in *SF3B1* and *EIF1AX*. As a further
349 drawback, the GEP approach intrinsically relies on differences observed within a cohort,
350 between multiple tumours. This makes this analysis less applicable to separate tumours, as
351 it always requires a comparison to other samples (or ‘normal’ values) to identify any
352 variation. For this reason, we further focussed on alternative approaches applicable to data
353 of individual uveal melanomas.

354

355 To better identify chromosomal alterations, we measured regionally-abundant allelic
356 imbalances of heterozygous common SNPs detectable in RNA data (**Figure 2**). This
357 approach has several similarities to a DNA-based methodology we presented and discussed
358 recently [31]. Based on (partial) copy number losses of chromosome 3, expressed loss of
359 heterozygosity could be observed at the transcriptional level and turned out to be an
360 excellent marker for this genetic event. The other way round, chromosome 8q copy number
361 increases, predominantly mono-allelic gains or amplifications, were also readily detected by
362 allelic imbalances present in RNA. Advantageously, by selecting SNPs known to be
363 frequently heterozygous in the population, no patient-matched genotype information was
364 required.

365

366 To detect BSE mutations at the RNA level, all mutational hotspot regions were screened and
367 possible transcriptional consequences of various alterations (i.e. alternative splicing) were
368 evaluated (**Figure 3**). Although a small number of mutations were missed due to insufficient
369 sequencing coverage, the large majority was successfully detected in the RNA data.
370 Interestingly, this included three additional *BAP1* mutations and five *EIF1AX* mutations in the
371 TCGA cohort that were previously unrecognised as part of the respective genes were not or
372 not sufficiently covered by the exome-captured DNA sequencing. Clinically, these alterations
373 are prognostically relevant and not to be missed in any routine mutational screening of a
374 uveal melanoma, substantiating complete coverage in any (targeted) sequencing panel. It is
375 also essential that these alterations are known and being taken into account when analysing
376 mutation data from these TCGA tumours in a research setting.

377
378 Though most mutations were directly recognised from nucleotide changes visible in the RNA
379 sequencing reads, a number of *BAP1* mutations were identified via unusual splicing events
380 within this gene (**Figure 3C and 4C**). In some tumours, the splice site disruption may be
381 directly caused by the mutation being located near a regular exon-intron boundary, or the
382 mutation introducing a novel splice site. Other tumours showed evidence of ‘nonsense-
383 associated alternative splicing’: (partial) exon skipping or intron retention, apparently in
384 response to the premature translation-termination codons introduced by nonsense or
385 frameshift mutations. In contrast to nonsense-mediated decay, in-frame alternative splicing
386 bypassing the original mutation might encode for a protein with saved functionalities, even
387 though the mutation is predicted to be truncating and highly pathogenic [33, 34]. Our
388 observations – possibly explainable by these phenomena, but yet to be followed up at a
389 functional level – further contribute to the notorious complexity of *BAP1* alterations and their
390 biological consequences [16, 17, 35-37].

391
392 Critically, our current study is limited by its low number of prospectively validated cases from
393 independent cohorts. Still, the cross-validation in a total of 85 tumours (i.e. the TCGA and
394 our own cohort combined) strongly suggests that most relevant alterations in uveal
395 melanoma can be detected at the transcriptional level, especially when various bioinformatic
396 approaches are combined. This indicates that RNA sequencing data, newly or
397 retrospectively collected for gene expression analysis, may be mined for genetic alterations
398 without the need to perform additional DNA-based measurements. Moreover, it may allow
399 researchers to study genotype-phenotype relations in the same tumour specimen in more
400 detail. This is particularly interesting in the context of measuring genetic heterogeneity next
401 to transcriptional heterogeneity, for example using multiregional or single-cell RNA
402 sequencing. Thirdly, the detectability of genetic alterations in the RNA of uveal melanomas

403 may provide the rationale to study (cell-free) RNA from liquid biopsies, which already
404 showed potential in other types of cancer [38-41].

405

406 In a follow-up study, our evaluations may be extended to other genetic alterations in uveal
407 melanoma. Besides chromosome 3 and 8q, (partial) copy number alterations affecting
408 chromosome 1, 6 and 16 are recurrently present and – although not extensively validated –
409 were already correctly observed as allelic imbalances in some of our tumours (**Figure 2 and**
410 **Supplementary Figure 1**). Additionally, mutations in splicing factor *SRSF2*, which seem to
411 form a rare alternative to *SF3B1* mutations [21, 42], might be recognised in the RNA
412 sequencing reads or by its own signature of alternative splicing. Moreover, it would be
413 therapeutically relevant to evaluate alterations involving *MBD4*. Biallelic inactivation of this
414 gene (via a mutation and copy number loss of its locus on chromosome 3) has been
415 identified as a rare cause of CpG>TpG hypermutation in uveal melanoma, conferring unique
416 sensitivity to immunotherapy [43, 44]. Next to identifying mutations at the RNA level,
417 additional evidence for *MBD4* inactivation can be found in an unusually high total mutational
418 burden, which might also be inferred from RNA sequencing data [45]. Finally, our
419 methodologies might be valuable beyond the field of uveal melanoma, and it would be
420 interesting to evaluate these in other types of cancer.

421

422 In conclusion, we developed and applied a variety of bioinformatic approaches showing that
423 transcriptional data – in addition to providing gene expression levels and profiles – forms a
424 rich source of (clinically-)relevant genetic information in uveal melanoma. Via RNA, valuable
425 insights could be obtained into the expressed genotype and its phenotypic consequences,
426 but this also demonstrated the vulnerabilities of an (insufficiently) targeted DNA
427 measurement. As illustrated by the identification of previously unreported mutations in the
428 thoroughly studied TCGA cohort, and the successful prospective analysis of tumours of our
429 own cohort, the analysis of transcriptional data may augment or even substitute current
430 DNA-based approaches, and has potential applicability in both oncological research and
431 clinical practice.

432 **Table**

433 **Table 1**

GEP	Mutations	Copy number alterations	Risk to (early) metastasis
Class I	Gα _q + <i>EIF1AX</i>		Low
	Gα _q + <i>SF3B1</i>	+8q	Intermediate
Class II	Gα _q + <i>BAP1</i>	-3, +8q	High

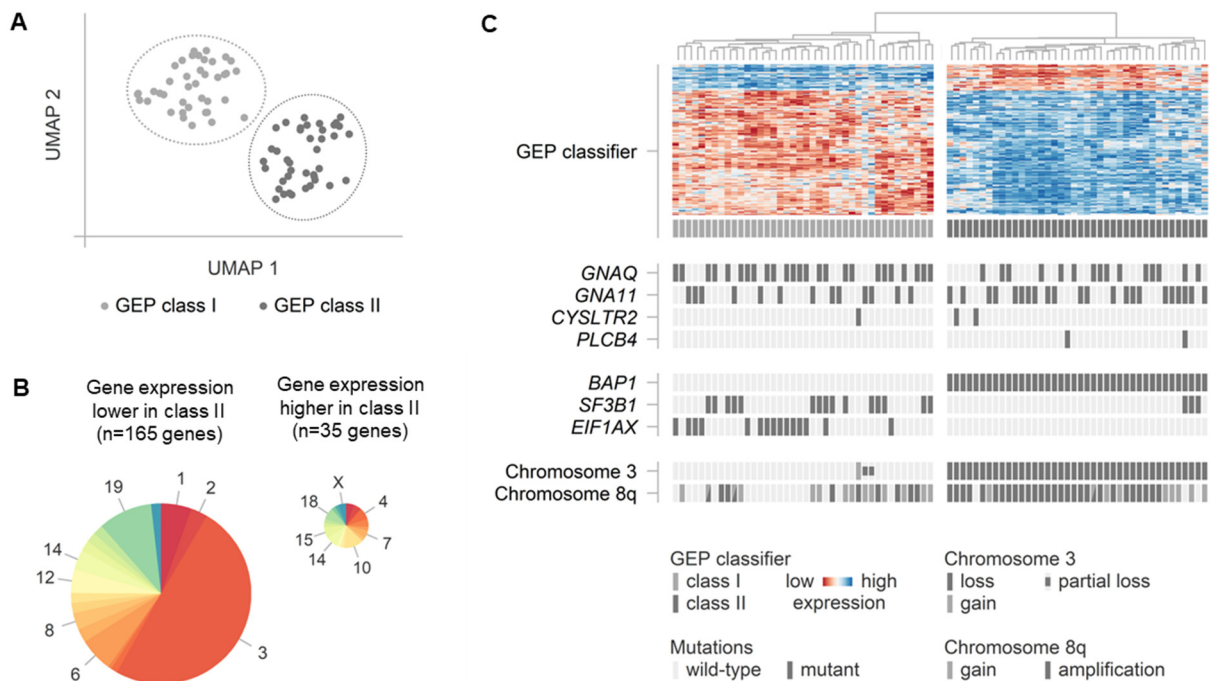
434

435 Summary of three most typical combinations of GEP classification, mutations, chromosomal
436 copy number alterations and their correlation to the risk of (early) metastatic dissemination
437 [1].

438

439 **Figures**

440 **Figure 1**



441

442

443 Cohort-wide gene expression profiling (GEP) to estimate the presence of genetic alterations
444 in our training cohort of uveal melanomas studied by The Cancer Genome Atlas (n=80).

445 (A) Two-dimensional uniform manifold approximation and projection (UMAP) analysis to
446 identify two clusters of tumours: GEP class I and II.

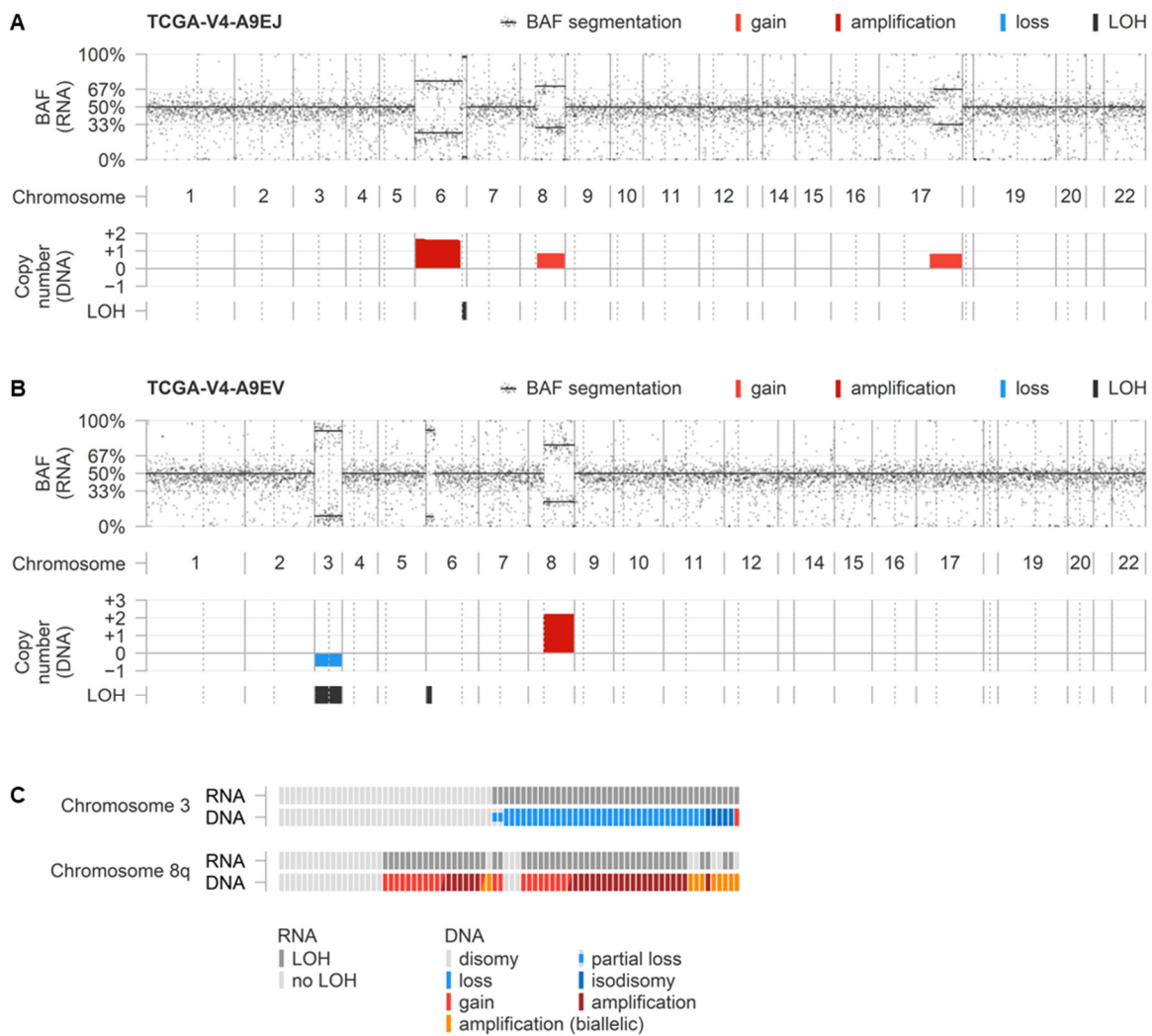
447 (B) Chromosomal location of signature genes characterising the two clusters.

448 (C) Relative gene expression levels of signature genes characterising the two clusters in
449 relation to the genetic alterations present per individual tumour.

450

451

452 **Figure 2**



453

454

455 RNA-inferred allelic imbalances in relation to DNA-confirmed copy number alterations.

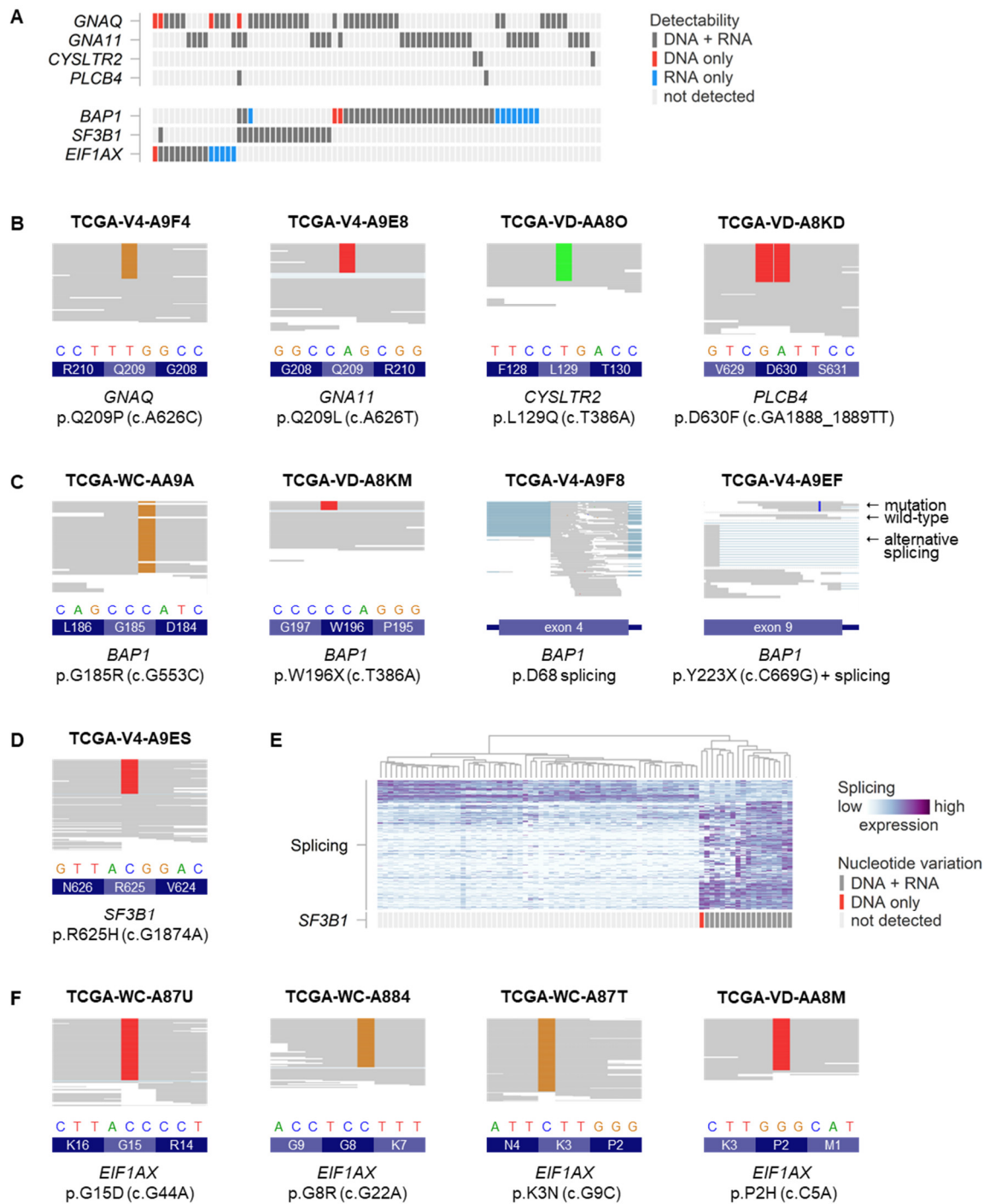
456 **(A)** Example of a tumour showing balanced expression of chromosome 3, but imbalanced
 457 expression of chromosome 8q, in line with a disomy 3 and copy number alteration of
 458 chromosome 8q. Additionally, alterations affecting chromosome 6p, 6q and 17q (partial) are
 459 correctly identified.

460 **(B)** Example of a tumour showing imbalanced expression of both chromosome 3 and 8q, in
 461 line with copy number alterations of the two chromosomes. Additionally, an alteration
 462 affecting chromosome 6p (partial) is correctly identified.

463 **(C)** Overview of RNA- and DNA-derived observations in the 80 TCGA tumours.

464

465 **Figure 3**



466

467

468 Detectability of mutations via RNA sequencing data in our training cohort of uveal
 469 melanomas studied by TCGA (n=80).

470 (A) Summary of detected mutations in comparison to findings in exome-captured DNA
 471 sequencing.

472 (B) Examples of detected $G\alpha_q$ signalling mutations in RNA sequencing data.

473 (C) Examples of detected *BAP1* mutations in RNA sequencing data: although some were
474 identified directly via nucleotide variation, others showed alternative splicing around the
475 mutant position.

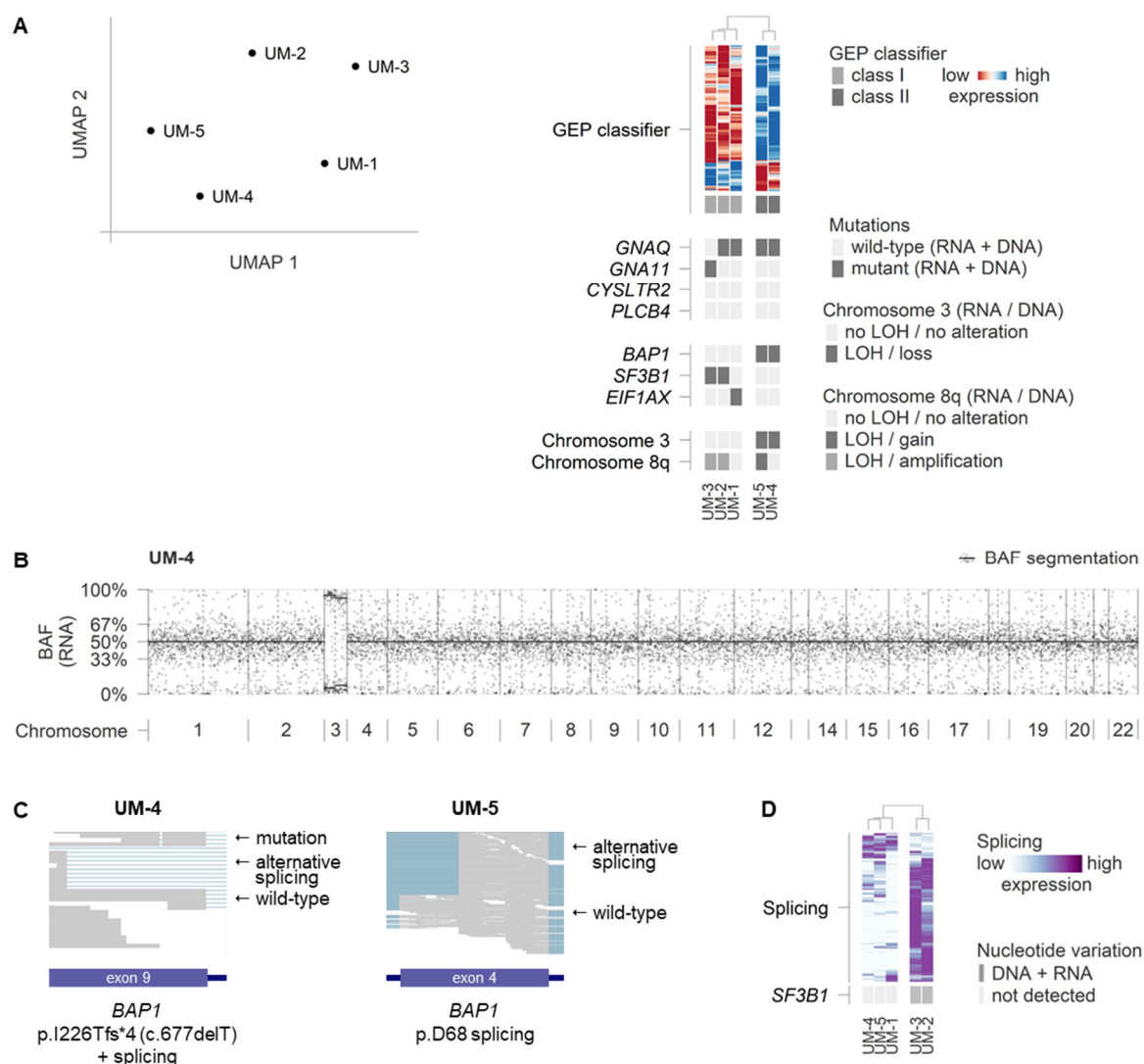
476 (D) Example of detected *SF3B1* mutation in RNA sequencing data.

477 (E) Analysis of a signature of alternative splicing to identify *SF3B1* mutant tumours.

478 (F) Examples of detected *EIF1AX* mutations in RNA sequencing data.

479

480 **Figure 4**



481

482 Analysis of our prospective cohort of uveal melanomas (n=5).

483 (A) Two-dimensional uniform manifold approximation and projection (UMAP) analysis of
484 cohort-wide gene expression profiling (GEP) and application of TCGA-derived GEP-classifier
485 in relation to the RNA- and DNA-based detectability of genetic alterations.

486 (B) Representative example of RNA-inferred allelic (im)balances to identify chromosomal
487 alterations. In this tumour, imbalanced expression of genes of chromosome 3 correctly
488 indicates the presence of a copy number alteration affecting this chromosome. In contrast,
489 no imbalance is observed on chromosome 8q, in line with a disomy 8q.

490 (C) *BAP1* alterations (mutations and mutation-associated alternative splicing) as observed in
491 the RNA sequencing data.

492 (D) Analysis of a signature of alternative splicing to identify *SF3B1* mutant tumours.

493 References

- 494 1. Jager, M.J., et al., *Uveal melanoma*. Nat Rev Dis Primers, 2020. **6**(1): p. 24.
- 495 2. Furney, S.J., et al., *SF3B1 mutations are associated with alternative splicing in uveal*
- 496 *melanoma*. Cancer Discov, 2013. **3**(10): p. 1122-1129.
- 497 3. Royer-Bertrand, B., et al., *Comprehensive Genetic Landscape of Uveal Melanoma by Whole-*
- 498 *Genome Sequencing*. Am J Hum Genet, 2016. **99**(5): p. 1190-1198.
- 499 4. Van Raamsdonk, C.D., et al., *Frequent somatic mutations of GNAQ in uveal melanoma and*
- 500 *blue naevi*. Nature, 2009. **457**(7229): p. 599-602.
- 501 5. Van Raamsdonk, C.D., et al., *Mutations in GNA11 in uveal melanoma*. N Engl J Med, 2010.
- 502 **363**(23): p. 2191-9.
- 503 6. Johansson, P., et al., *Deep sequencing of uveal melanoma identifies a recurrent mutation in*
- 504 *PLCB4*. Oncotarget, 2016. **7**(4): p. 4624-31.
- 505 7. Moore, A.R., et al., *Recurrent activating mutations of G-protein-coupled receptor CYSLTR2 in*
- 506 *uveal melanoma*. Nat Genet, 2016. **48**(6): p. 675-80.
- 507 8. Harbour, J.W., et al., *Frequent mutation of BAP1 in metastasizing uveal melanomas*. Science,
- 508 2010. **330**(6009): p. 1410-3.
- 509 9. Harbour, J.W., et al., *Recurrent mutations at codon 625 of the splicing factor SF3B1 in uveal*
- 510 *melanoma*. Nat Genet, 2013. **45**(2): p. 133-5.
- 511 10. Martin, M., et al., *Exome sequencing identifies recurrent somatic mutations in EIF1AX and*
- 512 *SF3B1 in uveal melanoma with disomy 3*. Nat Genet, 2013. **45**(8): p. 933-6.
- 513 11. Prescher, G., et al., *Chromosomal aberrations defining uveal melanoma of poor prognosis*.
- 514 Lancet, 1992. **339**(8794): p. 691-2.
- 515 12. Horsman, D.E. and V.A. White, *Cytogenetic analysis of uveal melanoma. Consistent*
- 516 *occurrence of monosomy 3 and trisomy 8q*. Cancer, 1993. **71**(3): p. 811-9.
- 517 13. Sisley, K., et al., *Abnormalities of chromosomes 3 and 8 in posterior uveal melanoma*
- 518 *correlate with prognosis*. Genes Chromosomes Cancer, 1997. **19**(1): p. 22-8.
- 519 14. White, V.A., et al., *Correlation of cytogenetic abnormalities with the outcome of patients with*
- 520 *uveal melanoma*. Cancer, 1998. **83**(2): p. 354-9.
- 521 15. Damato, B., et al., *Multiplex ligation-dependent probe amplification of uveal melanoma:*
- 522 *correlation with metastatic death*. Invest Ophthalmol Vis Sci, 2009. **50**(7): p. 3048-55.
- 523 16. Smit, K.N., et al., *Combined mutation and copy-number variation detection by targeted next-*
- 524 *generation sequencing in uveal melanoma*. Mod Pathol, 2018. **31**(5): p. 763-771.
- 525 17. Thornton, S., et al., *Targeted Next-Generation Sequencing of 117 Routine Clinical Samples*
- 526 *Provides Further Insights into the Molecular Landscape of Uveal Melanoma*. Cancers (Basel),
- 527 2020. **12**(4).
- 528 18. Tschentscher, F., et al., *Tumor classification based on gene expression profiling shows that*
- 529 *uveal melanomas with and without monosomy 3 represent two distinct entities*. Cancer
- 530 research, 2003. **63**(10): p. 2578-2584.
- 531 19. Zuidervaart, W., et al., *Gene expression profiling identifies tumour markers potentially playing*
- 532 *a role in uveal melanoma development*. Br J Cancer, 2003. **89**(10): p. 1914-9.
- 533 20. Onken, M.D., et al., *Gene expression profiling in uveal melanoma reveals two molecular*
- 534 *classes and predicts metastatic death*. Cancer Res, 2004. **64**(20): p. 7205-9.
- 535 21. Robertson, A.G., et al., *Integrative Analysis Identifies Four Molecular and Clinical Subsets in*
- 536 *Uveal Melanoma*. Cancer Cell, 2017. **32**(2): p. 204-220 e15.
- 537 22. de Lange, M.J., et al., *Heterogeneity revealed by integrated genomic analysis uncovers a*
- 538 *molecular switch in malignant uveal melanoma*. Oncotarget, 2015. **6**(35): p. 37824-35.
- 539 23. de Lange, M.J., et al., *Digital PCR-Based T-cell Quantification-Assisted Deconvolution of the*
- 540 *Microenvironment Reveals that Activated Macrophages Drive Tumor Inflammation in Uveal*
- 541 *Melanoma*. Mol Cancer Res, 2018. **16**(12): p. 1902-1911.
- 542 24. Alsafadi, S., et al., *Cancer-associated SF3B1 mutations affect alternative splicing by*
- 543 *promoting alternative branchpoint usage*. Nat Commun, 2016. **7**: p. 10615.
- 544 25. Field, M.G., et al., *Punctuated evolution of canonical genomic aberrations in uveal melanoma*.
- 545 Nat Commun, 2018. **9**(1): p. 116.
- 546 26. Karlsson, J., et al., *Molecular profiling of driver events in metastatic uveal melanoma*. Nat
- 547 Commun, 2020. **11**(1): p. 1894.
- 548 27. Nell, R.J., et al., *Involvement of mutant and wild-type CYSLTR2 in the development and*
- 549 *progression of uveal nevi and melanoma*. BMC Cancer, 2021. **21**(1): p. 164.

- 550 28. Taylor, A.M., et al., *Genomic and Functional Approaches to Understanding Cancer*
551 *Aneuploidy*. *Cancer Cell*, 2018. **33**(4): p. 676-689 e3.
- 552 29. Zoutman, W.H., R.J. Nell, and P.A. van der Velden, *Usage of Droplet Digital PCR (ddPCR)*
553 *Assays for T Cell Quantification in Cancer*. *Methods Mol Biol*, 2019. **1884**: p. 1-14.
- 554 30. Versluis, M., et al., *Digital PCR validates 8q dosage as prognostic tool in uveal melanoma*.
555 *PLoS One*, 2015. **10**(3): p. e0116371.
- 556 31. Nell, R.J., et al., *Allele-specific digital PCR enhances precision and sensitivity in the detection*
557 *and quantification of copy number alterations in heterogeneous DNA samples: an in silico and*
558 *in vitro validation study*. medRxiv, 2023: p. 2023.10.31.23297362.
- 559 32. van Essen, T.H., et al., *Prognostic parameters in uveal melanoma and their association with*
560 *BAP1 expression*. *Br J Ophthalmol*, 2014. **98**(12): p. 1738-43.
- 561 33. Cartegni, L., S.L. Chew, and A.R. Krainer, *Listening to silence and understanding nonsense:*
562 *exonic mutations that affect splicing*. *Nat Rev Genet*, 2002. **3**(4): p. 285-98.
- 563 34. Mohn, F., M. Buhler, and O. Muhlemann, *Nonsense-associated alternative splicing of T-cell*
564 *receptor beta genes: no evidence for frame dependence*. *RNA*, 2005. **11**(2): p. 147-56.
- 565 35. Repo, P., et al., *Population-based analysis of BAP1 germline variations in patients with uveal*
566 *melanoma*. *Hum Mol Genet*, 2019. **28**(14): p. 2415-2426.
- 567 36. Niersch, J., et al., *A BAP1 synonymous mutation results in exon skipping, loss of function and*
568 *worse patient prognosis*. *iScience*, 2021. **24**(3): p. 102173.
- 569 37. Cole, Y.C., et al., *Correlation between BAP1 Localization, Driver Mutations, and Patient*
570 *Survival in Uveal Melanoma*. *Cancers (Basel)*, 2022. **14**(17).
- 571 38. Krug, A.K., et al., *Improved EGFR mutation detection using combined exosomal RNA and*
572 *circulating tumor DNA in NSCLC patient plasma*. *Ann Oncol*, 2018. **29**(3): p. 700-706.
- 573 39. Schoofs, K., et al., *Comprehensive RNA dataset of tissue and plasma from patients with*
574 *esophageal cancer or precursor lesions*. *Sci Data*, 2022. **9**(1): p. 86.
- 575 40. Albrecht, L.J., et al., *Circulating cell-free messenger RNA enables non-invasive pan-tumour*
576 *monitoring of melanoma therapy independent of the mutational genotype*. *Clin Transl Med*,
577 2022. **12**(11): p. e1090.
- 578 41. Albitar, M., et al., *Combining cell-free RNA with cell-free DNA in liquid biopsy for hematologic*
579 *and solid tumors*. *Heliyon*, 2023. **9**(5): p. e16261.
- 580 42. van Poppel, N.M., et al., *SRSF2 Mutations in Uveal Melanoma: A Preference for In-Frame*
581 *Deletions?* *Cancers (Basel)*, 2019. **11**(8).
- 582 43. Rodrigues, M., et al., *Outlier response to anti-PD1 in uveal melanoma reveals germline MBD4*
583 *mutations in hypermutated tumors*. *Nat Commun*, 2018. **9**(1): p. 1866.
- 584 44. Johansson, P.A., et al., *Prolonged stable disease in a uveal melanoma patient with germline*
585 *MBD4 nonsense mutation treated with pembrolizumab and ipilimumab*. *Immunogenetics*,
586 2019. **71**(5-6): p. 433-436.
- 587 45. Katzir, R., N. Rudberg, and K. Yizhak, *Estimating tumor mutational burden from RNA-*
588 *sequencing without a matched-normal sample*. *Nat Commun*, 2022. **13**(1): p. 3092.
- 589